Studies of a novel conducting polymer by cyclic and square wave voltammetries: Its synthesis and characterization

Fabiana D'Eramo*, María Alicia Zón, Héctor Fernández,
Leonides Sereno, Alejandro Heraldo Arévalo

*Departamento de Química, Facultad de Ciencias Exactas, Físico-Químicas y Naturales, Universidad Nacional de Río Cuarto,
Agencia Postal No. 3, 5800 Río Cuarto, Córdoba, Argentina*

ARTICLE INFO

ABSTRACT

A novel conducting polymer of polynaphthidine, poly(NAP), was synthesized electrochemically by direct anodic oxidation of naphthidine in aqueous media. The yield of the electropolymerization reaction depends on the temperature and pH of the solution. It was possible to differentiate two working regions: I (for pH < 0.5 and all temperatures) where the film yield tends to zero and II (for approximately 2.0 < pH < 2.8 and temperatures >15 °C) where the film production is maximum. Therefore, the naphthidine electrooxidation mechanism was studied under experimental conditions of region I by cyclic (CV) and square wave voltammetries (SWV) as well as by controlled potential electrolysis.

The experimental conditions of region II were chosen to obtain the poly(NAP). The electrochemical response of the film was investigated in pH 1 $HClO_4$ + 0.1 M $NaClO_4$ electrolyte solution by CV and SWV. A plot of $I_{p,n}/f$ vs. f from SW voltammograms showed the so-called "quasi-reversible maximum". Formal potential, formal rate constant and anodic transfer coefficient for the surface redox process were also evaluated from the SWV.

The poly(NAP) is insoluble in common organic solvents and shows electrochromic behaviour. Its probable structure was determined by FTIR spectroscopy.

© 2008 Elsevier Ltd. All rights reserved.

1. Introduction

It is well known that properties of conducting polymers strongly depend on their structural characteristics. Therefore, many efforts have been made in the field of the synthesis of both, new monomers and polymers with the aim to obtain materials with suitable characteristics for potential applications in electrochemistry and some other sciences [1–3]. Electro-oxidative polymerization of new monomers with concurrent polymer film deposition has been considered as an effective and versatile route for modification of an electrode surface by organic polymeric compound.

During the past quarter century, the most widely studied conducting polymer was polyaniline because of its potential applications in rechargeable batteries, electrochromic, display devices, supercapacitors, antistatic coating, biosensors, etc. [4,5]. A reaction mechanism for the anodic oxidation of anilines, leading to head-to-tail, head-to-head and tail-to-tail dimmers, as well as to polymeric products, with the participation of electrogenerated cation radicals, has been previously proposed [6,7]. However, the study of

this polymer is highly complicated due to the existence of two different redox forms, with the possibility of protonation and/or oxidation reactions which allow the passage from a form to another one. On the other hand, the main objective of basic research in the polyaniline system has been to investigate properties of substituted polyanilines [8–10]. The goal of this research has been to introduce substituents on to the polyaniline backbone which enhance the desirable properties of polyaniline. Substituent groups placed on the phenyl ring of polyaniline have been found to yield the best results in this respect [11–15]. However, literature search reveals that there is another much less tested but equally interesting possibility, the electropolymerization of the dinuclear aromatic amines [1,16–19]. We have previously reported the electrooxidation of polynuclear amines such as 1-napthylamine and 4,4′-diamine-biphenyl (benzidine) in aqueous solutions and 1,1′-binaphthalene 4,4′-diamine (naphthidine) (NAP) in non-aqueous media [20–24]. In general, it has been found that the behaviour of these polynuclear amines follows general rules of mononuclear amines. The overall electrode process follows a mechanism of ECE type [25,26]. The films obtained in each case showed different structural characteristics and properties, determined not only by the monomer type that originated them, but also by the nature of the solvent and the proton concentration in the reaction medium. In addi-

tion, these new conducting polymers show some advantageous properties such as, high chemical stability in aqueous solution and air, good redox reversibility and broad potential window, wide pH range of application without evident degradation, capacity to pre-concentrate species in solution and easy preparation and strong attachment to the electrode surface [23,24,27–30].

Due to the interesting properties that show this kind of novel conducting polymers and considering that the main propose of our investigation group is to show the electroanalytical usefulness of these materials, we report in this paper the preparation of a film, poly(NAP), produced by the electrochemical oxidation of NAP in aqueous solution. This reaction medium was chosen because of the most of analytical determinations reported in literature have been principally carried out in this medium. The probable mechanism of the polymerization process is discussed by combining cyclic (CV) and square wave voltammetries (SWV) and controlled potential electrolysis.

In this respect, the SWV is particularly a fast and sensitive technique for the detection of the amount of initially adsorbed analyte by considering its ability to discriminate against capacitive currents [31]. In addition, SW voltammograms of surface redox processes are highly sensitive to the kinetics of the charge transfer [32,33]. They are characterized by both, the so-called "quasi-reversible maximum", where the ratio between the peak current and the frequency is approximately a parabolic function of the kinetic parameter κ, and by the splitting of the voltammetric peak with the amplitude at a given frequency [34–36]. According to the theory, the maxima of these parabolic functions and the splitting of the voltammetric peak can be used to calculate the formal rate constant, the transfer coefficient, the number of electrons exchanged and the formal potential of redox couples immobilized on the electrode surface [34–37].

Therefore, the thermodynamic and kinetics parameters of the NAP film electrogenerated are measured from SWV experiments by combining the results of quasi-reversible maximum and the splitting of the voltammetric peak on the SW amplitude at a given frequency methods.

Moreover, in order to improve the performance of this new conjugated polymer, basic studies on the variables that affect the deposition and redox properties of film are evaluated.

2. Experimental

The monomer employed for the electropolymerization, NAP (**I**) [22] from ICN Biomedicals Inc., was used as received. All the other reagents were analytical grade unless otherwise stated.
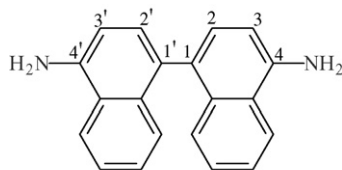
(**I**)

Ultra pure water was obtained from LABCONCO equipment model 90901-01 (HPLC grade water). The solutions used to obtain the film were prepared by weighted amounts of NAP and dissolved in an acidic supporting electrolyte solution. All the experiments were carried out under inert nitrogen atmosphere. The pH was changed by the addition of an acid or a base as it was necessary. The pH was measured in situ with an Orion 8104 Ross (pH 0–14) combination electrode. The working temperature was controlled using a LAUDA K4R thermostat-cryostat. The temperature was varied from 10 to 35 °C.

Electrochemical experiments were performed by using an Auto-Lab PGSTAT 30 potentiostat, run with GPES software, version 4.9 (Eco Chemie, Utrech, The Netherlands). Working electrodes were a Pt wire or a Pt disk (area, A = 0.31 and 0.018 cm², respectively). Before each experiment the Pt disk was polished mechanically with wet alumina power (0.3 and 0.05 μm, from Fischer) and then, it was rinsed with distilled water and sonicated for 15 min to remove residual polishing material. The Pt wire was flame burnt. The counter and the reference electrodes were a Pt wire of large area ($A \cong 2$ cm²) and a saturated calomel electrode (SCE), respectively. All potentials are referred to the aqueous SCE.

The scan rate (v) in cyclic voltammograms was varied from 0.002 to 0.200 V s⁻¹. The voltammograms were corrected for IR drop by positive feedback technique.

Characteristic parameters used for diffusion controlled SW voltammograms were pulse-half-peak-to-peak (ΔE_{SW}) = 25 mV; staircase step height (ΔE_s) = 5 mV and the square wave frequency (f) was varied in the range from 10 to 100 Hz. SW voltammograms were fitted by using the COOL algorithm [38]. Background currents were substrated by using a home made programme. SW parameters used to study the film surface redox process were ΔE_s = 5 mV; ΔE_{SW} and f were varied in the range from 25 to 200 mV and from 8 to 60 Hz, respectively.

In situ spectroelectrochemical studies on polymer were performed using a spectroelectrochemical cell consisting of an optically transparent indium tin oxide (ITO)-coated glass as working electrode, Ag/AgCl and platinum wire as reference and counter electrodes, respectively. UV–vis spectra were obtained with a Hewlett-Packard 8452A spectrophotometer. The infrared absorption spectra were recorded in the range of 500–4000 cm⁻¹ using a Nicolet 5-5XLFTIR Spectrophotometer by the KBr pellet method at a resolution of 4 cm⁻¹ for 120 scans.

3. Results and discussion

3.1. Electrochemical oxidation of the NAP monomer

The oxidation of NAP is a reversible process whose potential E^0 is given by the average value of the anodic peak potential $E_{p,aI}$ (peak I) and the cathodic peak potential $E_{p,cII}$ (peak II); that means E^0 = (0.55 + 0.52)/2 = 0.54 V, Fig. 1a. A certain yellow substance was produced at the electrode surface. This couple could be assigned to the formation of the dication of NAP through the following quasi-reversible processes as is discussed below:

$$NAP \overset{k^o_{f1}}{=\!=} NAP^{\bullet+} + 1e^- \tag{1}$$

$$NAP^{\bullet+} \overset{k^o_{f2}}{=\!=} NAP^{++} + 1e^- \tag{2}$$

where $NAP^{\bullet+}$ and NAP^{++} are the radical monocation and the dication of NAP, respectively. In addition, the NAP $E_{p,aI}$ is lower than that of 1-naphtylamine ($E_{p,a}$ = 0.700 V) [20] and benzidine ($E_{p,a}$ = 0.600 V) [21], which are structurally related to NAP. This fact could be explained by considering that a more extended π system is present in NAP than in 1-naphtylamine and benzidine, which would stabilized the radical monocation and the dication of NAP in a greater extension, making easier the NAP electrochemical oxidation. The second and further potential scans (see inset in Fig. 1a) showed a new peak system in the potential range from 0 to 0.50 V (peaks III/IV). This peak system shows the characteristic behaviour of a surface electroactive substance. The progressive increase in the peak current values for both, peaks III and IV, suggests the continuous build-up of a polymeric electroactive film, poly(NAP), on the working electrode surface.
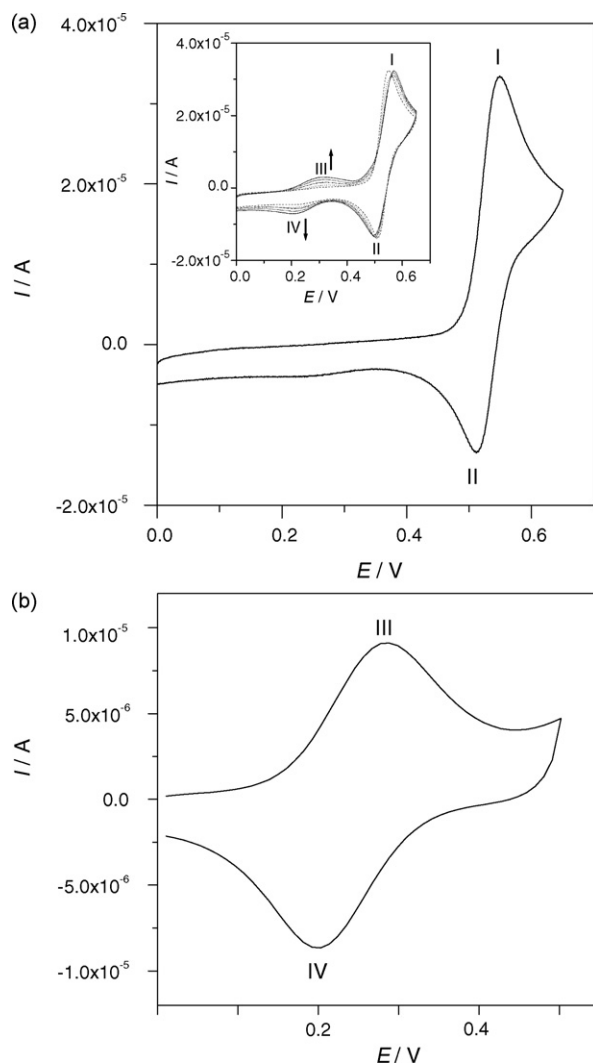
Fig. 1. (a) Cyclic voltammogram of NAP at pH 2.5 and 0.025 V s^{-1}, in HClO$_4$ + 0.1 mol L^{-1} NaClO$_4$ aqueous solution at a Pt wire electrode (A = 0.31 cm^2); c_{NAP} = 5 × 10^{-4} mol L^{-1}; T = 20 °C. Inset consecutive cyclic voltammograms. (b) Electrochemical response of poly(NAP) film in pH 1 HClO$_4$ + 0.1 mol L^{-1} NaClO$_4$ aqueous solution: v = 0.050 Vs^{-1}; T = 20 °C.

In addition, a visual inspection of the electrode surface showed the formation of a visible film on the electrode which was initially blue in colour and then became black as the deposit material amount was increased. As a consequence of the film formed on the electrode surface, the oxidation of NAP detected in the first cycle at 0.55 V was shifted to a more positive potential and a decrease in currents of peaks I/II was observed in consecutive scans. These results provide information about the increase of the resistance in the polymer film and the over-potential need to over-come that resistance (see below) [39].

To confirm the existence of a film on the electrode surface the experiment showed in Fig. 1a was repeated under strong nitrogen bubbling in order to clarify whether the species responsible for the III/IV peaks are attached to the electrode surface or are in the vicinity of the electrode surface. Under these experimental conditions, peaks III/IV appeared and peak currents increased slowly during the consecutive potential scans. This behaviour was also confirmed when the electrode was cycled in a free amine solvent-supporting electrolyte medium. A typical voltammogram for the poly(NAP) film obtained under this conditions is shown in Fig. 1b. Its redox
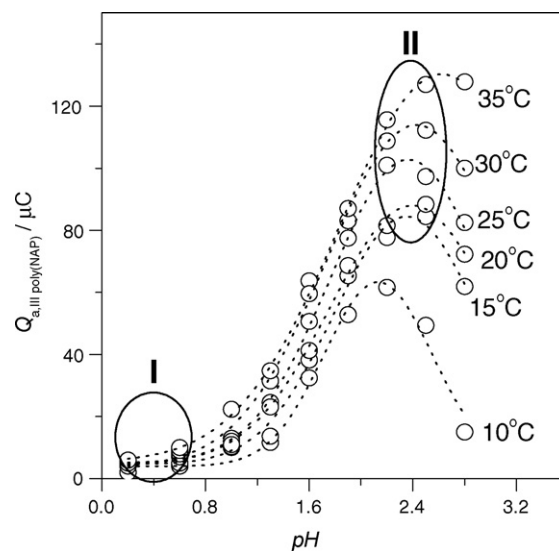
Fig. 2. Yield of electropolymerization reaction with pH and T. c_{NAP} = 5 × 10^{-4} mol L^{-1}, Pt wire electrode (A = 0.31 cm^2); v = 0.025 Vs^{-1}. Poly(NAP) anodic charge measured at pH 1 HClO$_4$ + 0.1 mol L^{-1} NaClO$_4$ aqueous solution: v = 0.050 Vs^{-1}; T = 20 °C.

response showed an oxidation and a reduction peak centred at about 0.29 and 0.20 V, respectively, putting clearly in evidence the electroactive nature of this surface redox couple.

The electropolymerization reaction yield showed a dependence with temperature and pH of the solution. Therefore, systematic studies were performed varying these parameters in order to obtain the optimum conditions for the electropolymerization reaction. The film was always prepared by cycling the potential 15 times at the same potential interval showed in Fig. 1a. The same procedure was used for films prepared at different pH and temperatures. Then, films were rinsed with supporting electrolyte solution to remove the excess NAP and transferred to another cell containing only an electrolyte solution (pH 1 HClO$_4$ + 0.1 mol L^{-1} NaClO$_4$), where studies about films were carried out. The amount of poly(NAP) deposited on the electrode surface, which can be expressed as the electropolymerization reaction yield, was determined from its anodic charge (peak III). The net charge was calculated by subtracting from the total charge the corresponding background value. The anodic charge was plotted as a function of pH for each temperature at which the film was obtained. Results are shown in Fig. 2.

As can be seen, when the temperature was increased the charge increased, indicating that the overall process for film formation followed a normal Arrhenius behaviour. When the pH was increased the film yield reached a maximum, which showed dependence with the temperature. Then, the film yield decreased, which could be indicating that another reaction would be competing with the film formation.

From Fig. 2, it is possible to differentiate two working regions: I (for pH < 0.5 at all temperatures) and II (for approximately 2.0 < pH < 2.8 at temperatures > 15 °C). In region I, the film yield tended to zero, while the film production was maximum in region II. On the basis of these results, the NAP electrooxidation mechanism without any surface complication was studied under experimental conditions of region I, where the coupled chemical reaction to the film formation was minimized. On the contrary, the experimental conditions of region II were chosen to obtain the maximum yield for the electropolymerization reaction. Then, studies related to films were performed at pH 1 HClO$_4$ + 0.1 mol L^{-1} NaClO$_4$ electrolyte solution in the absence of NAP at 20 °C.

3.1.1. Studies performed at pH 0.5

3.1.1.1. Cyclic voltammetry and controlled potential electrolysis.

When experiments of CV are carried out at pH 0.5 the current response that is obtained is similar to that shown in Fig. 1a, with the exception that the film formation is not detected. A separation between the anodic and cathodic peak potentials ($E_{p,aI} - E_{p,cII}$) of 0.031 V was found at 0.050 V s^{-1}, being this value close to the theoretical one predicted for a two-electron Nernstian redox couple, i.e. 0.030 V at 25 °C [40,41]. Moreover, the ratio between cathodic and anodic peak currents ($I_{p,cII}/I_{p,aI}$) determined by using the method proposed by Nicholson [42] was very close to 1, indicating the presence of a Nernstian wave with a stable reaction product under these experimental conditions.

Behaviours of $I_{p,aI}$ and $E_{p,aI}$ were studied at different scan rates. No $E_{p,aI}$ shift was observed when the v was varied from 0.002 to 0.100 V s^{-1}, as it is theoretically expected [40,43]. A plot of $I_{p,aI}$ vs. $v^{1/2}$ was linear showing a diffusion control for the electrode process. This behaviour was observed for all NAP concentrations studied, i.e. from 1×10^{-4} to 5×10^{-4} mol L^{-1}. The highest NAP concentration studied was limited by the monomer solubility in this reaction medium. The same behaviour mentioned on $I_{p,aI}$ vs. $v^{1/2}$ plots was observed at the different temperatures studied (10–35 °C), with an increase in slope values as the temperature was increased, as it is theoretically expected. In addition, it was also found that $I_{p,aI}$ varied linearly with the c_{NAP} in the range from 0.5×10^{-4} to 5×10^{-4} mol L^{-1}. From $I_{p,aI}$ vs. c_{NAP} plots, a value of 3.65×10^{-6} cm^2 s^{-1} was calculated for the diffusion coefficient of NAP (D_{NAP}) at 25 °C by using $n = 2$ [40].

These results would be indicating that the oxidation process is consistent with two successive monoelectronic charge transfers to give the NAP dication, where the second electron transfer is much easier then the first one [41]. These results are similar to those obtained for benzidine [21] and NAP studied in our laboratory in aqueous and non-aqueous media, respectively [22].

Controlled potential electrolysis was performed in order to confirm the number of electron exchange in the redox process under those experimental conditions. Therefore, solutions of NAP at pH 0.5 were electrolyzed at 0.60 V on a Pt electrode of large area ($A = 8$ cm^2). The apparent electron number (n_{app}) per molecule of electrolyzed substance was obtained by plotting ln I vs. t [44]. A linear relationship was observed up to 15% conversion, giving a value of $n_{app} \cong 2$.

3.1.1.2. Square wave voltammetry.

The forward (I_f), reverse (I_r) and net (I_n) currents obtained from a typical SW voltammogram after background currents subtraction are shown in Fig. 3. The best fitting curves for net, forward and reverse currents (solid lines in Fig. 3) were obtained when the two-electron quasi-reversible dimensionless current function was chosen to perform the fitting. After the
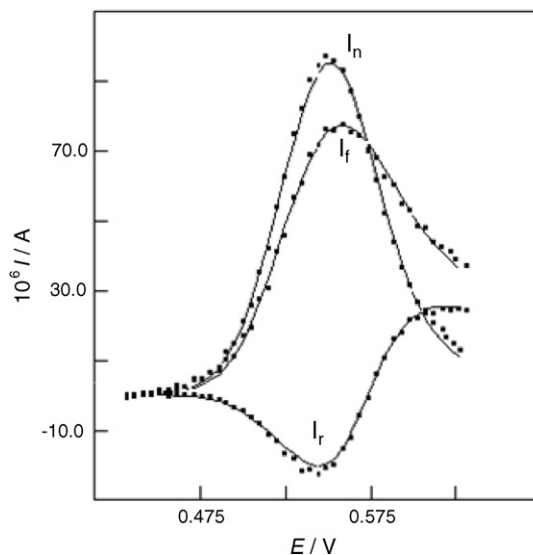
Fig. 3. Square wave voltammograms for oxidation of 2×10^{-4} mol L^{-1} of NAP at pH 0.5 in HClO$_4$ + 0.1 mol L^{-1} NaClO$_4$ aqueous solution. Forward (I_f), reverse (I_r) and net (I_n) experimental currents are shown by squares while the corresponding currents from the best fitting are shown by solid lines. Working electrode: Pt disk, $A = 0.018$ cm^2, $\Delta E_{SW} = 25$ mV, $\Delta E_s = 5$ mV and $f = 20$ Hz.

most probable mechanism was identified, calculations were carried out with a 95% confidence level.

The net currents responses showed a constant peak width of 64 mV in the frequency range studied, value close to that expected theoretically for a two-electron reversible reaction, i.e. 63 mV at 25 °C [38,43]. The voltammetric half wave potential ($E_{1/2} \approx E_f^0$), k_f^0 and $(1 - \alpha)$ for an overall two-electron process can be obtained from SW voltammograms using a non-linear least square analysis through the COOL algorithm [38]. For reaction controlled by semi-infinite diffusion conditions, the slope, (a), of the linear regression between experimental and dimensionless currents is:

$$a = nFAD_{NAP}^{1/2}c_{NAP}(\pi t_p)^{-1/2} \tag{3}$$

where n is the electron number exchanged, F the Faraday constant, t_p the characteristic time, i.e. the pulse width of the excitation waveform and the other terms were previously defined.

When a quasi-reversible electrochemical reaction is chosen as the mechanistic model for performing the fit, the COOL algorithm gives the best values of $E_{1/2}$, $(1 - \alpha)$ and the dimensionless function $\log(\kappa' t_p^{1/2})$, which is related to the heterogeneous charge transfer

Table 1

Results of the best fitting obtained from the individual forward and reverse square wave voltammograms from data corresponding to a solution of $c_{NAP} = 2 \times 10^{-4}$ M in pH 0.5 HClO$_4$ + NaClO$_4$ aqueous medium on a platinum disk electrode ($A = 0.018$ cm^2)[a]

f (Hz)	$E_{1/2}$ (V)	$(1-\alpha)$	$\log(\kappa' t_p^{1/2})$	Slope[b] (μA)	κ'	$(1-r)$[c] ($\times 10^4$)	χ^2[d] ($\times 10^{14}$ μA)
10	0.554	0.13	−0.3187	53.4	2.15	3.95	8.75
20	0.550	0.20	−0.2213	72.7	3.80	6.56	35.0
30	0.539	0.29	−0.3029	92.6	3.86	12.0	108.0
40	0.542	0.31	−0.3197	108.4	4.28	9.70	117.0
60	0.545	0.30	−0.3406	129.9	5.00	7.71	128.0
80	0.541	0.27	−0.3183	155.6	6.08	8.03	189.0
100	0.542	0.36	−0.3967	179.0	5.67	13.42	414.0

[a] Reference electrode: SCE. Temperature: 25 °C.

[b] Ratio between experimental and dimensionless currents.

[c] Complement of correlation coefficient of experimental vs. dimensionless currents linear regression.

[d] χ^2: chi^2 function.

rate constant through:

$$\kappa' = \frac{k_f^o}{D^{1/2}} \tag{4}$$

by assuming that the diffusion coefficient for the reduced and oxidized species are taken as equal [38].

Characteristic values of $E_{1/2}$, $(1 - \alpha)$ and $\log(\kappa' t_p^{1/2})$ for NAP in pH 0.5 $HClO_4 + 0.1$ mol L^{-1} $NaClO_4$ aqueous solution obtained from the best fitting curves for individual forward and reverse currents, which are more sensitive to the kinetic effects than net currents [45,46] are reported in Table 1. Besides, results of fitting performed on net currents did not differ significantly from those obtained when the fitting was carried out on forward and reverse currents, as expected for a system not complicated by complex reaction mechanisms [46].

The fits were very good, as can be inferred from the complement of the correlation coefficient $(1 - r)$ of the linear regression between experimental and dimensionless currents and the chi^2 (χ^2) function values (see Table 1), two parameters which measure the quality of fitness. From the fitting results, an average value of $\kappa' = 4 \pm 1$ was calculated. A plot of a vs. $t_p^{-1/2}$ (Eq. (3)) was linear when the fitting was performed on forward and reverse currents ($r = 0.9982$). From the slope of this plot, a value of $D_{NAP} = 3.7 \times 10^{-6}$ cm^2 s^{-1} was determined, being this value in excellent agreement with that value previously obtained for D_{NAP} from CV. It was then used to obtain the overall rate constant for the two-electron process by using Eq. (4), i.e. $k_f^o = 0.009$ cm s^{-1}. Average values of $E_{1/2}$ and $(1 - \alpha)$ calculated for the overall electrode process with the corresponding standard deviations were: (0.545 ± 0.003) V and (0.27 ± 0.08), respectively. The apparently odd results obtained for $(1 - \alpha)$ and κ' at a frequency of 10 Hz may be explained by considering that the experimental system would be moving from quasi-reversible to nearly reversible behaviour for that long measurement time [46], although a definitive conclusion is not known yet. The statistical Q-test (at 90% confidence level) performed on $(1 - \alpha)$ and κ' values showed that these values did not have to be rejected.

3.1.2. Studies performed in the $2.0 < pH < 2.8$ range

As mentioned above, the maximum yield of the electropolymerization reaction can be obtained in the 2–2.8 pH range and $T > 15\,°C$ (see Fig. 2). The pH clearly affects the cyclic voltammogram of NAP/NAP^{++} couple. Specifically, we have observed two main changes when the pH increases; first, the potential range where NAP is oxidized is shifted to more negative values and second, a change in the peak current ratio $I_{p,cII}/I_{p,aI}$, i.e., it is lower than one.

On the other hand, as it can be observed in Fig. 4a, the NAP anodic charge (Q_{NAP}) was independent from pH, on the contrary, cathodic charge continuously decreased as the pH increased. These results would be indicating that the NAP^{++} concentration at the electrode–solution interface decreases as the pH increases, suggesting that this species it is not stable. Obviously, this observed pH-influence indicates that following chemical reactions involving protons should be coupled with the two-electron electrochemical reaction. This assumption is also supported by the observed behaviour of the NAP oxidation current (peak I), at pH 2.5 and $25\,°C$, when the sweep rates and NAP concentration are varied. It was found that the experimental current function ($I_{pa,I}/C_{NAP}Av^{1/2}$) decreases with the square root of the scan rate ($v^{1/2}$) and depends on the monomer concentration as shown in Fig. 4b. These results confirm that a chemical reaction would be coupled to the initial charge transfer step, which may have higher than first-order kinetics [26].
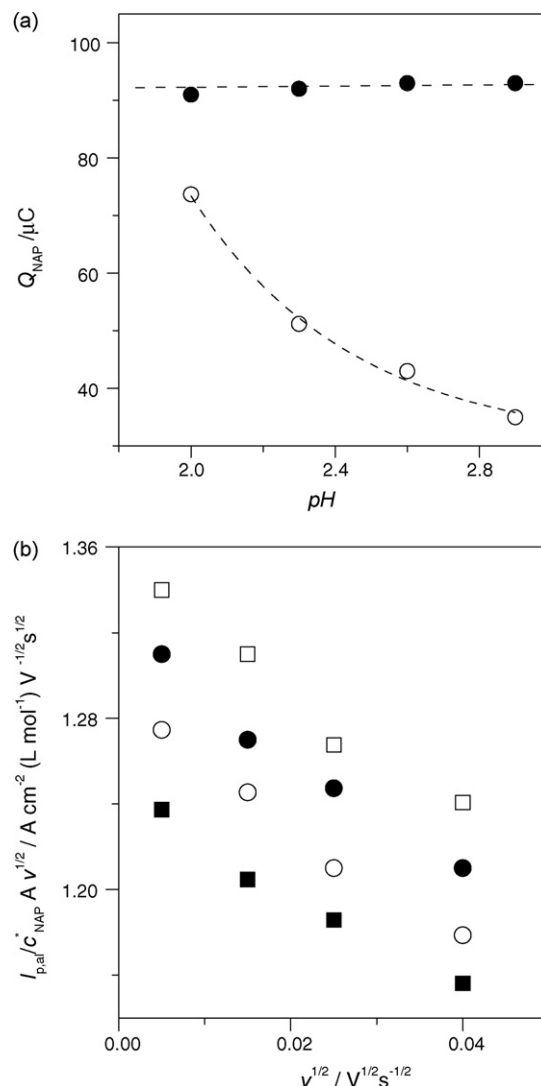
Fig. 4. (a) Correlation of Q_{NAP} whit pH in $HClO_4 + 0.1$ mol L^{-1} $NaClO_4$ aqueous solution: (●) anodic and (○) cathodic charges. Pt wire electrode ($A = 0.31$ cm^2); $v = 0.025$ Vs^{-1} and $T = 20\,°C$. (b) Correlation of $I_{p,aI}/c_{NAP} A v^{1/2}$ with square root of the scan rate for different c_{NAP} at pH 2.5 $HClO_4 + 0.1$ mol L^{-1} $NaClO_4$ aqueous solution: (□) 2.15×10^{-4} mol L^{-1}; (●) 2.96×10^{-4} mol L^{-1}; (○) 3.65×10^{-4} mol L^{-1}; (■) 4.5×10^{-4} mol L^{-1}.

### 3.1.2.1. Studies of the surface redox couple by cyclic voltammetry.

According to the results presented above, the poly(NAP) is prepared by repetitive cycling at a rate of 0.05 V s^{-1} between 0.0 and 0.65 V in a pH 2.5 $HClO_4 + 0.1$ mol L^{-1} $NaClO_4$ aqueous solution containing a c_{NAP} of 5×10^{-4} mol L^{-1}. The electrochemical response of poly(NAP) in monomer free 0.1 M $HClO_4 + 0.1$ mol L^{-1} $NaClO_4$ aqueous solution have a characteristic response, as shown in Fig. 1b. Reversible redox peaks, attributed to a proton/electron addition/elimination reactions at the –NH– sites in the polymeric film, are clear. It should be noted that films obtained under these conditions have a peak system much simpler than other known electroactive films such as those of polyanilines [8–10].

The study of the effect of v shows that anodic (III) and cathodic (IV) peak currents vary linearly with v between 0.002 and 0.150 V s^{-1} as predicted theoretically for adsorbed species or film-modified electrodes with thin-layer behaviour [40,47]. In addition, both peak current values are similar. For values of v above 0.200 V s^{-1} semi-infinite diffusion behaviour is observed. These

effects of v on I_p depend on the film thickness and are characteristic of a redox modified electrode.

On the other hand, both anodic and cathodic peaks of the film have similar shapes with a peak potential difference ($E_{p,aIII} - E_{p,cIV}$) of about 0.080 V, which is independent from v. Values of the peak potentials are also independent of the sweep rate between 0.002 and 0.150 V s^{-1}. Anodic and cathodic peaks have a width at half-height maximum slightly greater than 0.091 V at 25 °C, value expected for a thin-layer cell with Nernstian behaviour for $n = 1$ [40]. If we assume this model to explain the behaviour of poly(NAP), combining the charge involved in either the voltammetric oxidation ($Q_{a,III}$) or reduction ($Q_{c,IV}$) peaks with the slope of the respective plot I_p $vs.$ v (i.e., $nFQ/4RT$), it is possible to estimate a value of 0.7 for the apparent number of electrons exchanged in the redox sites (see also results of SWV below, Section 3.1.2.2). A molecular interpretation of this value would imply the knowledge of the film redox reaction. However, it could be interpreted as a function of interactions between redox sites [22] or even surface heterogeneity [48]. The charges $Q_{a,III}$ and $Q_{c,IV}$ for the anodic and cathodic redox processes are quite similar when the measurement is performed under conditions of thin-layer behaviour. According to these results, all quantitative studies were performed only when these conditions were satisfied. $Q_{a,III}$, measured as previously indicated, is proportional to the number of cycles involved in the film formation (Fig. 5), this fact could be interpreted as homogeneous growth of the film. Besides, it was found that the electronic resistance of the surface redox couple increases as the poly(NAP) anodic charge increases (see inset in Fig. 5). The electronic resistance of the film was measured by following the Pickup et al. method [49], by dipping the Pt/film electrode into a mercury pool, and measuring the current through the film as a function of applied voltage. The electrode was immersed in the mercury at open circuit for ca. 10 min before measurements were made. Linear Ohm's law plots were obtained between 0.0 and 0.200 V for poly(NAP).

3.1.2.2. Studies of the surface redox couple by square wave voltammetry.

I_f, I_r and I_n currents obtained from SW voltammograms of the surface redox couple, recorded in supporting electrolyte solution (pH 1 HClO$_4$ + 0.1 mol L^{-1} NaClO$_4$) as the reaction medium, are shown in Fig. 6. These results put clearly in evidence the surface nature of this electrochemical signal. If the adsorption of both, the reactant and the product of a quasi-reversible surface redox couple is equally strong, a plot of the net peak current frequency ratio ($I_{p,n}$)/f $vs.$ f or $1/f$ shows a maximum, which appears at the SW frequency which is approximately equal to the standard (formal) rate constant (k_s) of the redox reaction [33,35]. A plot of $I_{p,n}/f$ $vs.$ f is shown in Fig. 7, where $I_{p,n}$ values are the average of five replicated experiments. The ratio between the net peak current and frequency
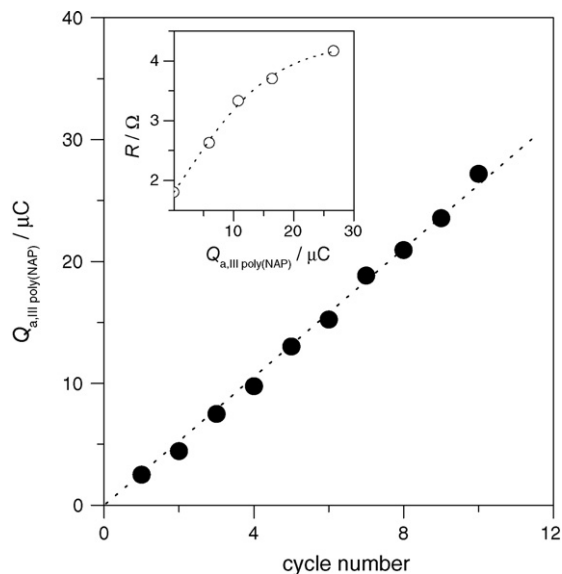
Fig. 5. Correlation between the anodic charge of poly(NAP) and the number of potential cycles employed in the production of the film: $c_{NAP} = 5 \times 10^{-4}$ mol L^{-1} at pH 2 in HClO$_4$ + 0.1 mol L^{-1} NaClO$_4$ aqueous solution at 0.025 V s^{-1}. Pt wire electrode ($A = 0.31$ cm^2) and $T = 20$ °C. Film charge measured at pH 1, $T = 20$ °C and $v = 0.050$ Vs^{-1}. Inset: the variation of the electronic resistance of poly(NAP), R, with different anodic charge of the film.

reached a maximum at an average maximum frequency (f_{max}) of (11 ± 1) Hz.

On the other hand, the relationship between the maximum kinetic parameter (κ_{max}) and k_s can be expressed as [33,35]

$$k_s = \kappa_{max} f_{max} \qquad (5)$$

where κ_{max} depends on the transfer coefficient, $(1 - \alpha)$, and on the product of the SW amplitude and the number of electron, $n\Delta E_{SW}$, but it is independent of the normalized potential increment, $n\Delta E_S$, and of the amount of initially adsorbed reactant [35].

As the anodic transfer coefficient of the surface redox couple is not known, at this stage of the work, an average parameter $\bar{\kappa}_{max}$, which is applied for $0.1 < (1 - \alpha) < 0.9$, can be used to obtain k_s (see Table 2 in [36]). Besides, as the apparent electron number exchanged in the redox sites is nearly one, as it was previously inferred from cyclic voltammograms, k_s could be only estimated as 14 s^{-1} by using the critical kinetic parameter $\kappa_{max} = (1.25 \pm 0.07)$, which apply for $0.1 < (1 - \alpha) < 0.9$ and $n\Delta E_{SW}$ equal to 25 mV [36].

On the other hand, the combination of the "quasi-reversible maximum" and the "split SW net peak" methods [50] can be used to

Table 2
Anodic ($I_{pa,III}$) and cathodic ($I_{pc,IV}$) peak currents, anodic ($E_{pa,III}$) and cathodic ($E_{pc,IV}$) peak potentials for the spitted SW peaks, the overall E_f^o and $(1 - \alpha)$ values for the surface redox couple of poly(NAP) at pH 1 HClO$_4$ + NaClO$_4$ aqueous medium on a platinum disk electrode ($A = 0.018$ cm^2)

f (Hz)	ΔE_{SW} (mV)	$I_{pa,III}$ (μA)	$I_{pc,IV}$ (μA)	$E_{pa,III}$ (V)	$E_{pc,IV}$ (V)	E_f^o (V)	$(1 - \alpha)$
	75	18.51	15.5	0.244	0.273	0.258	0.45
	100	20.99	19.12	0.229	0.283	0.256	0.47
	125	22.47	21.32	0.215	0.293	0.254	0.48
10	150	23.15	22.45	0.200	0.308	0.254	0.49
	175	23.16	22.6	0.181	0.322	0.251	0.49
	200	21.94	21.94	0.166	0.342	0.254	0.50
	225	19.6	19.63	0.142	0.356	0.249	0.50
	150	70	62.2	0.215	0.298	0.256	0.46
40	175	71.3	63.7	0.195	0.317	0.256	0.47
	200	69.7	60.5	0.181	0.332	0.256	0.46

$\overline{E_f^o} = (0.254 \pm 0.003)$ V, $\quad (\overline{1 - \alpha}) = (0.48 \pm 0.02)$.
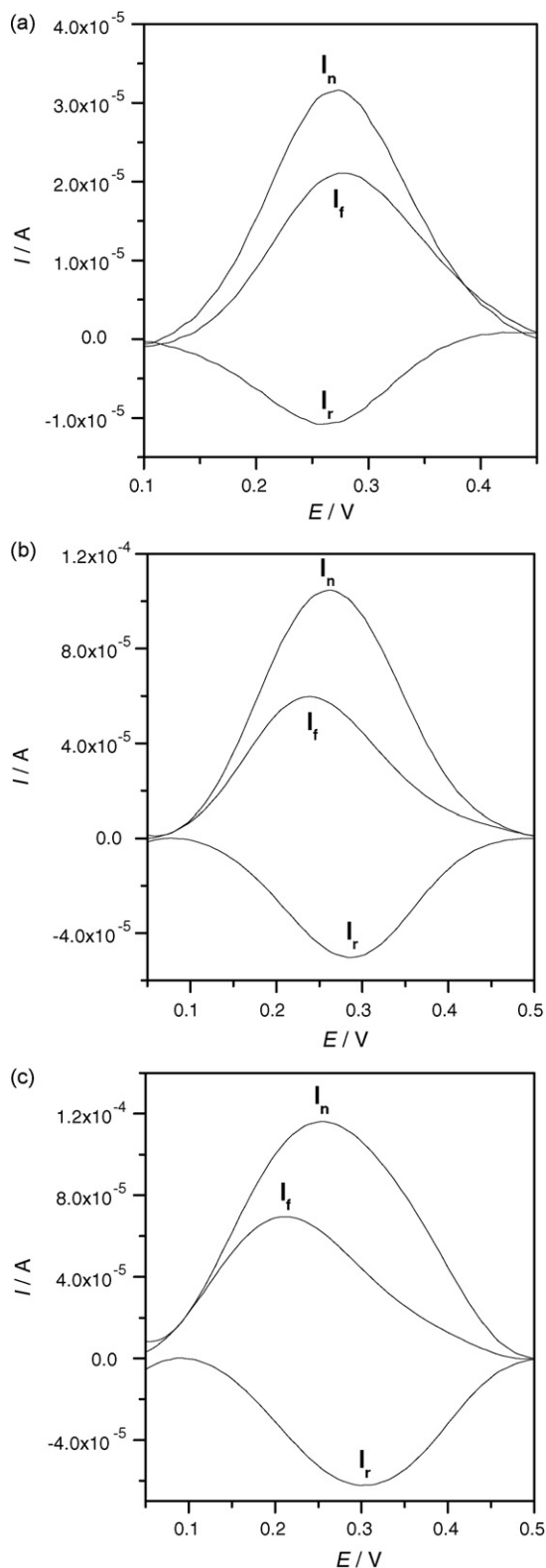
Fig. 6. The forward (I_f), reverse (I_r) and net (I_n) currents from SW voltammograms recorded at different SW amplitudes. (a) $\Delta E_{SW} = 25$ mV; (b) $\Delta E_{SW} = 100$ mV and (c) $\Delta E_{SW} = 150$ mV, at pH 1 in $HClO_4 + 0.1$ mol L^{-1} NaClO$_4$ aqueous solution, $\Delta E_s = 5$ mV and $f = 40$ Hz.
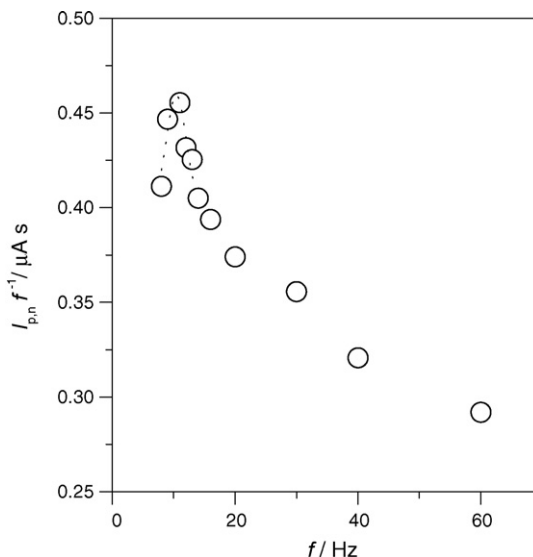
Fig. 7. Dependence of the ratio between net peak currents and frequency ($I_{p,n} f^{-1}$) and the SW frequency at pH 1 in $HClO_4 + 0.1$ mol L^{-1} NaClO$_4$ aqueous solution, $\Delta E_s = 5$ mV and $\Delta E_{SW} = 25$ mV.

obtain the exchange electron number, n, the anodic transfer coefficient, $(1 - \alpha)$ and the formal rate constant, k_s, as it is discussed below.

As reported elsewhere, changes in the peak shapes, which carry kinetics information, are more effectively produced by varying the SW amplitude than by varying the frequency [34]. Thus, a set of SWV experiments where SW amplitude was varied at a given frequency was performed. These representative voltammograms showing net, forward and reverse currents performed at a $f = 40$ Hz and at different ΔE_{SW} are shown in Fig. 6. As it is theoretically predicted [34,36], large changes in voltammogram shape were obtained as ΔE_{SW} was increased at a given frequency. For small ΔE_{SW} (i.e., 25 mV) and $f = 40$ Hz, only a narrow net peak was observed (Fig. 6a). However, the peak started to widen as ΔE_{SW} is increased (Fig. 6b and c). The occurrence of widen peak is due to the relationship between the potential-dependent rate constant for the surface redox process and the time scale of the experiment. An average value of (0.254 ± 0.003) V was estimated for the formal potential ($\overline{E_f^0}$) of the adsorbed redox couple by considering that, both, the forward and reverse peaks are symmetrically located about the formal potential of the surface redox couple [34]. Values of the anodic and cathodic peak potentials as well as the average value obtained for the formal potential of the surface redox couple are shown in Table 2.

The peak separation (ΔE_p) of the split net SW responses of fast and chemically reversible surface redox reaction has been proposed to depend on the product $n\Delta E_{SW}$ as well as on the kinetic parameter κ. This dependence can be expressed by [51]:

$$\Delta E_p (mV) = 2n\Delta E_{SW} - (50 - 5\kappa) \tag{6}$$

where the influence of $(1 - \alpha)$ on ΔE_p is not significant [51].

Plots of ΔE_p vs. ΔE_{SW} at frequencies of 10 and 40 Hz were linear ($r = 0.9973$ and $r = 0.9995$, respectively). An average value of the slope with the corresponding standard deviation of (1.32 ± 0.05) was obtained from these plots. Therefore, the apparent number of electrons exchanged in the redox sites was determined to be 0.66, in good agreement with that value previously determined from CV experiments (see Section 3.1.2.1).

On the other hand, the form of the net SW voltammogram for adsorbed reversible redox couples is strongly influenced by the

transfer coefficient [34,51]. For $(1 - \alpha) > 0.2$, the ratio between the forward (anodic) and reverse (cathodic) peak currents, $(I_{pa,III}/I_{pc,IV})$, can be approximated by a single exponential curve [51]:

$$\frac{I_{pa,III}}{I_{pc,IV}} = 5.6414 \exp[-3.4606(1 - \alpha)] \qquad (7)$$

Values of $I_{pa,III}$ and $I_{pc,IV}$ obtained at different ΔE_{SW} and $f = 10$ and 40 Hz are shown in Table 2. An average value of (0.48 ± 0.02) was calculated for $(1 - \alpha)$ from experimental data through Eq.(7).

Finally, the k_s value was determined combining both methods, i.e., the "quasi-reversible maximum" and "the split SW peak" through Eq.(5). $f_{max} = (11 \pm 1)$ Hz was taken from the first method and $\kappa_{max} = 1.19$ was extracted from Table 1 in Ref. [36] by considering values calculated from the second method, i.e. $(n\Delta E_{SW} = 25$ mV) and $(1 - \alpha) = 0.5$. Therefore, one can calculate $k_s = (13 \pm 1) \, s^{-1}$ which agrees very closely to that calculated from "quasi-reversible maximum" method (see above).

3.1.2.3. Properties and structure of the surface redox couple. Interesting properties of poly(NAP) films were observed:

 (i) Poly(NAP) films are insoluble in common organic solvents such as acetonitrile, dimethylformamide, dimethylsulphoxide, dichloromethane and hexane. This fact could be indicating a stiff structure and probably having a high molar mass, precluding any study of the film in solution.
 (ii) Poly(NAP) films retain their electrochemical activity even when they are left in the air or dipped in aqueous solutions for long a time.
(iii) The film redox behaviour is dependent on the pH of the electrolyte solution. It has a reproducible behaviour in the pH range from 1 to 4, but at pH values ≥ 5, practically no response is observed. However, at these pH values the film is not destroyed and its original redox response can be recovered when the pH is restored to 1. This fact would be indicating that protons and electrons take part in the electrode reaction of poly(NAP). It is also important to emphasize that in spite of the monomer that produces poly(NAP) is a derivative of aniline, this polymer shows an advantage respect to polyaniline films because of it can be used directly on a wide pH range without evident degradation.
(iv) Poly(NAP) films has electrochromic properties. It is colourless in the reduced state at 0.0 V and light blue in the oxidized state at 0.50 V (Fig. 8a). The absorbance of the film at reduced state shows the UV band related to the π–π^* transition of the basic aromatic structure of NAP at the wavelength region from 320 to 360 nm. As the film is progressively oxidized there is a decrease in absorbance in this region. An increase in absorbance at wavelength region from 450 to 800 nm is observed which correspond to the oxidized form of the polymer. This behaviour is similar to that observed during the oxidative doping of other conducting polymers, such as polybenzidine [21] and polyaniline [52] and it is reversible, i.e. when the oxidized film is reduced the initial spectrum is recovered.

All these characteristics of poly(NAP) allow several possibilities of application of these materials, which are being investigated more deeply in our laboratory.

Other important question to solve is the kind of coupling existing between the monomer species. In order to further explore the poly(NAP) structure the IR absorption spectrum of NAP together with the spectra of the polymer was recorded (Fig. 8b). In the monomer spectrum two absorption peaks due to the N–H stretching vibrations of the amino groups were observed at ~3399 (1) and ~3312 cm^{-1} (2), a strong absorption peak corresponding to the
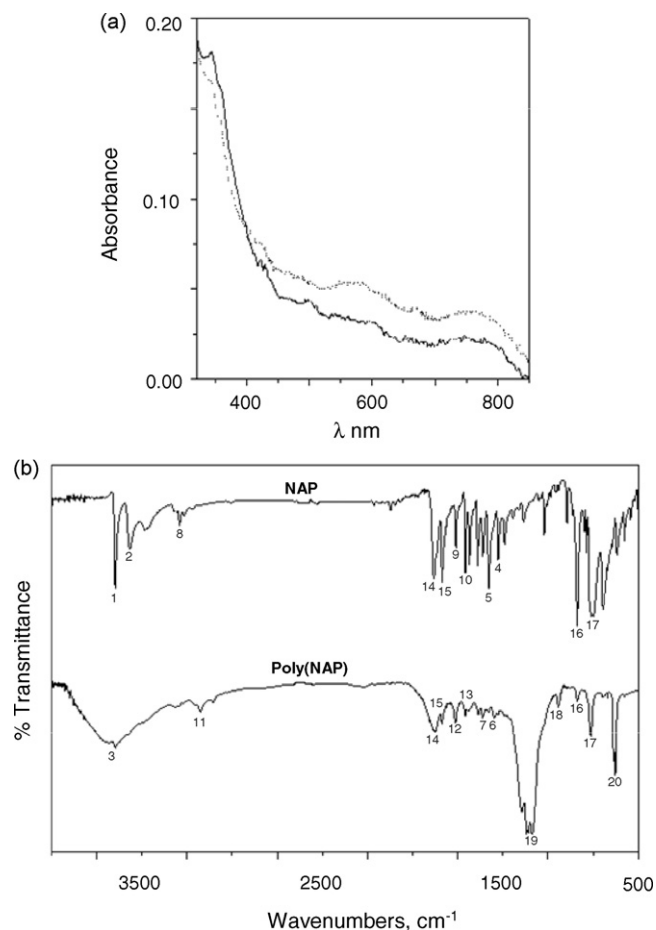
Fig. 8. (a) UV–vis spectra of poly(NAP) on an ITO electrode at pH 1 in HClO$_4$ + 0.1 mol L^{-1} NaClO$_4$ aqueous solution at (—) 0 mV and (…) 500 mV. (b) FTIR spectra of NAP and its electropolymerized film poly(NAP).

N–H stretching vibrations of the imino groups of the poly(NAP) was observed at ~3460 cm^{-1} (3). This fact suggests that the NH$_2$ groups take part in the electropolymerization. The C–N stretching bands, which are characteristic of an aromatic amine, were observed at 1270 (4) and 1326 cm^{-1} (5) for the NAP and at ~1301 (6) and 1365 cm^{-1} (7) for the polymer sample [53,54]. The absorption peaks at ~3042 cm^{-1} (8) and ~1510 (9)–1464 cm^{-1} (10) in the NAP spectrum are considered to be due to the stretching vibration mode of the C–H and C=C bands present in the aromatic ring, respectively [54]. These absorption peaks were recorded at ~2930 cm^{-1} (11) and 1500 (12)–1460 cm^{-1} (13) in the poly(NAP) spectrum. The absorption peaks observed at ~1637 (14) and 1586 cm^{-1} (15) for both the monomer and the polymer are characteristic of bending vibration of N–H bonds. The comparative study of the NAP and poly(NAP) FTIR spectra in the low-frequency region 650–1000 cm^{-1}, corresponding to the aromatic C–H out-of-plane deformation vibrations, γ(C–H), reveals changes of the aromatic substitution pattern. In the monomer spectrum two bands appear at 848 (16) and 746 cm^{-1} (17) due to the γ(C–H) vibrations of two and four adjacent H atoms of the fused benzene rings, respectively. The intensity decreased in the first band respect to the second one in the spectrum of poly(NAP) indicates that some coupling reactions between the amino group of one NAP moiety and the carbon 3 (3′) of other monomer may occur. On the basis of these results, a new band at 936 cm^{-1} (18) in the spectrum of the polymer are attributable to the γ(C–H) vibration of one isolated ring H atom.

Finally, the bands at about 1092 (19) and 634 cm^{-1} (20) which are present only for the polymer spectrum, are assigned to the presence of ClO$_4^-$ anion [53].

4. Conclusion

A novel conducting polymer, poly(NAP), was electrochemically synthesized in aqueous solution by direct anodic oxidation of NAP. Studies of CV as well as SWV and controlled potential electrolysis demonstrate that the electrooxidation of NAP in acidic media leads to the formation of the dication, NAP^{++}, by an EE process where the second electron transfer is much easier than the first one. At pH < 0.5 and all temperatures tested the NAP peak current ratio, $I_{pc,II}/I_{pa,I}$, was close to 1 indicating that the dication is stable under these experimental conditions. At higher pH, only the NAP anodic charge ($Q_{a,I}$) remained unaltered, while a diminution of the NAP cathodic charge ($Q_{c,II}$) and the current peak ratio ($I_{pc,II}/I_{pa,I}$) when the pH increases were observed. These facts imply that the pH change affects the NAP^{++} stability and as consequence favours a coupled chemical reaction to give a polymer film following the two-electron transfer. The dependence of the current function with NAP concentration shows that the dication reacts following a kinetic law of order higher than one to form probably a dimmer which may induce the polymerization reaction. From the fitting of the experimental cyclic and square wave voltammograms, performed at pH < 0.5, employing a quasi-reversible redox reaction model the formal rate constant ($k_f^o = 0.009$ cm s^{-1}), an average values of $E_{1/2} = (0.545 \pm 0.003)$ V and $(1 - \alpha) = (0.27 \pm 0.08)$, were obtained for the overall two-electron electrode process.

Poly(NAP) film has a voltammetric peak system much simpler than other known electroactive films such as polyaniline. This film shows a thin-layer behaviour at sweep rates lower than 0.150 V s^{-1}, while at higher rates semi-infinite diffusion behaviour is observed.

From the square wave voltammograms an average values for the formal potential $\bar{E}_f^o = (0.254 \pm 0.003)$ V and for $(1 - \alpha) = (0.48 \pm 0.02)$ for poly(NAP) were estimated. The $k_s = (13 \pm 1)$ s^{-1} value was determined by combining both methods the "quasi-reversible maximum" and the "split SW peak".

Poly(NAP) exhibits interesting properties: it is insoluble in common organic solvents, retain its electrochemical activity even when it is left in the air or dipped in aqueous solutions for long a time, it has electrochromic properties and it has a reproducible behaviour in the pH range from 1 to 4. At pH higher than 5 its response is lost but it is recovered when the medium is acidified. The future work will be focused to study these properties and its applications.

Acknowledgments

References

[1] K.M. Ismail, Z.M. Khalifa, M.A. Azzem, W.A. Badawy, Electrochim. Acta 47 (2002) 1867.
[2] S.-M. Chen, Y.-H. Fa, J. Electroanal. Chem. 553 (2003) 63.
[3] M.C. Blanco-López, M.J. Lobo-Castañón, A.J. Miranda-Ordieres, P. Tuñón-Blanco, Trends Anal. Chem. 23 (2004) 36.
[4] C. Li, S. Mu, Synth. Met. 144 (2004) 143.
[5] A.A. Hermas, M. Nakayama, K. Ogura, Electrochim. Acta 50 (2005) 2001.
[6] A.F. Díaz, J.A. Logan, J. Electroanal. Chem. 111 (1980) 111.
[7] R. Noufi, A.J. Nozik, J. White, L.F. Warren, J. Electrochem. Soc. 129 (1982) 2261.
[8] J. Yue, Z.H. Wang, K.R. Cromack, A.J. Epstein, A.G. MacDiarmid, J. Am. Chem. Soc. 113 (1991) 2665.
[9] A. Malinauskas, R. Holze, J. Solid State Electrochem. 3 (1999) 429.
[10] C.Y. Chung, T.C. Wen, A. Gopalan, Electrochim. Acta 47 (2001) 423.
[11] Y.W. Park, J.S. Moon, M.K. Bak, J.I. Jin, Synth. Met. 29 (1989) E389.
[12] R.L. Clark, S.C. Yang, Synth. Met. 29 (1989) E337.
[13] L.H. Dao, M. Leclerc, J. Guay, J.W. Chevalier, Synth. Met. 29 (1989) E377.
[14] A.A. Athawale, B.A. Deore, V.V. Chobukswar, Mater. Chem. Phys. 58 (1999) 94.
[15] F.A. Viva, E.M. Andrade, F.V. Molina, M.F. Florit, J. Electrochem. Soc. 471 (1999) 180.
[16] K. Chiba, T. Ohsaka, N. Oyama, J. Electroanal. Chem. 217 (1987) 239.
[17] M. Abdel-Azzem, U.S. Yousef, D. Limosin, G. Pierre, J. Electroanal. Chem. 417 (1996) 163.
[18] M.R. Nateghi, M.H. Mosslemin, H. Hadjimohammadi, React. Funct. Polym. 64 (2005) 103.
[19] G. Ćirić-Marjanović, M. Trchová, P. Matějka, P. Holler, B. Marjanović, I. Juranić, React. Funct. Polym. 66 (2006) 1670.
[20] A.H. Arévalo, H. Fernández, J.J. Silver, L. Sereno, Electrochim. Acta 35 (1990) 741.
[21] F. D'Eramo, A.H. Arévalo, J.J. Silber, L. Sereno, J. Electroanal. Chem. 382 (1995) 85.
[22] A.H. Arévalo, H. Fernández, J.J. Silber, L. Sereno, Electrochim. Acta 35 (1990)731.
[23] H. Fernández, A.H. Arévalo, L. Sereno, Bol. Soc. Chil. Quím. 43 (1998) 107.
[24] F. D'Eramo, A.H. Arévalo, in: H. Fernández, M.A. Zón (Eds.), Recent Developments and Applications of Electroanalytical Chemistry, Research Signpost, Kerala, India, 2002, p. 5.
[25] N. Vettorazzi, J.J. Silber, L. Sereno, J. Electroanal. Chem. 158 (1983) 89.
[26] N. Vettorazzi, J.J. Silber, L. Sereno, J. Electroanal. Chem. 125 (1981) 459.
[27] F. D'Eramo, J.M. Marioli, A.H. Arévalo, L. Sereno, Electroanalysis 11 (1999)481.
[28] F. D'Eramo, J.M. Marioli, A.H. Arévalo, L. Sereno, Talanta 61 (2003) 341.
[29] F. D'Eramo, L. Sereno, A.H. Arévalo, Electroanalysis 18 (2006) 1523.
[30] F. D'Eramo, L. Sereno, A.H. Arévalo, Electroanalysis 19 (2007) 96.
[31] J. Osteryoung, J. O'Dea, in: A.J. Bard (Ed.), Electroanalytical Chemistry, vol. 14, Marcel Dekker, New York, 1986, p. 209.
[32] M. Lovrić, S. Komorsky-Lovrić, J. Electroanal. Chem. 248 (1988) 239.
[33] S. Komorsky-Lovrić, M. Lovrić, Z. Fresenius, Anal. Chem. 335 (1989) 289.
[34] J.J. O'Dea, J.G. Osteryoung, Anal. Chem. 65 (1993) 3090.
[35] Š. Komorsky-Lovrić, M. Lovrić, J. Electroanal. Chem. 384 (1995) 115.
[36] S. Komorsky-Lovrić, M. Lovrić, Electrochim. Acta 40 (1995) 1781.
[37] V. Mirceski, M. Lovric, Electroanalysis 11 (1999) 984.
[38] J.J. O'Dea, J. Osteryoung, T. Lane, J. Phys. Chem. 90 (1986) 2761.
[39] T.F. Otero, E.D. Larreta-Azelain, Polymer 29 (1988) 1522.
[40] A.J. Bard, L.R. Faulkner (Eds.), Electrochemical Methods: Fundamentals and Applications, 2nd ed., Wiley, New York, 2001.
[41] D.S. Polcyn, I. Shain, Anal. Chem. 38 (1966) 370.
[42] R.S. Nicholson, Anal. Chem. 38 (1966) 1406.
[43] K.B. Oldham, J.C. Myland, Fundamentals and Electrochemical Science, Academic Press, London, 1994, p. 420.
[44] D.H. Geske, A.J. Bard, J. Phys. Chem. 63 (1959) 1057.
[45] J.G. Osteryoung, R.A. Osteryoung, Anal. Chem. 57 (1985) 101A.
[46] J.J. O'Dea, K. Wikiel, J. Osteryoung, J. Phys. Chem. 94 (1990) 3628.
[47] J. Schreurs, E. Barendrecht, Recl. Trav. Chim. Pays-Bas. 103 (1984) 205.
[48] T. Komura, S. Isogai, T. Yamaguchi, K. Takahashi, J. Electroanal. Chem. 490 (2000) 70.
[49] J. Ochmanska, P.G. Pickup, J. Electroanal. Chem. 271 (1989) 83.
[50] V. Mirceski, M. Lovrić, B. Jordanoski, Electroanalysis 11 (1999) 660.
[51] V. Mirceski, M. Lovrić, B. Jordanoski, Electroanalysis 9 (1997) 1283.
[52] E.M. Genies, M. Lapkowski, C. Tsinavis, New J. Chem. 12 (1988) 181.
[53] F.A. Miller, C.H. Wilkins, Anal. Chem. 24 (1952) 1253.
[54] G. Socrates, Infrared Characteristic Group Frequencies, Tables and Charts, 2nd ed., Wiley, New York, 1994.